Available online at www.sciencedirect.com
ScienceDirect
Journal of Catalysis 249 (2007) 370–379
JOURNAL OF CATALYSIS
www.elsevier.com/locate/jcat

Methanation of carbon dioxide on Ni-incorporated MCM-41 catalysts: The influence of catalyst pretreatment and study of steady-state reaction

Guoan Du [a], Sangyun Lim [a], Yanhui Yang [b], Chuan Wang [a], Lisa Pfefferle [a], Gary L. Haller [a,*]

[a] *Department of Chemical Engineering, Yale University, P.O. Box 208286, New Haven, CT 06520-8286, USA*
[b] *School of Chemical and Biomedical Engineering, Nanyang Technological University, Singapore 639798, Singapore*

Received 3 January 2007; revised 23 March 2007; accepted 29 March 2007

Available online 21 June 2007

Abstract

The methanation of carbon dioxide was carried out over Ni-incorporated MCM-41 catalysts. The Ni-MCM-41 catalysts containing 1–3 wt% Ni were prepared by incorporating the Ni ions into the framework of siliceous MCM-41 with the procedure developed in our previous work [S. Lim, G.L. Haller, J. Phys. Chem. B 106 (2002) 8437]. Pretreatment using pure H_2 at different temperatures affected the reactivity. Pretreatment at 973 K for 0.5 h was the best among the conditions tested. At this temperature, the Ni was mostly reduced but remained highly dispersed. Significant selectivity to methane (85.1%) was obtained with 1 wt% Ni-MCM-41 at a reaction temperature as low as 573 K and gas hourly space velocity (GHSV) of 5760 $\mathrm{l\,kg^{-1}\,h^{-1}}$ under atmospheric pressure. Higher selectivity (96.0%) and space-time yield (91.4 $\mathrm{g\,kg^{-1}\,h^{-1}}$) were achieved with higher Ni loading catalysts (3 wt% Ni) at the same space velocity. This selectivity was maintained at higher temperature (673 K) with increased space-time yield (633 $\mathrm{g\,kg^{-1}\,h^{-1}}$). The X-ray absorption result demonstrates that the Ni particle size does not significantly change during reaction.

Keywords: Ni-MCM-41; N_2 physisorption; XRD; H_2-TPR; CO chemisorption; X-ray absorption spectroscopy; XANES; EXAFS; Space time yield (STY)

1. Introduction

The catalytic hydrogenation of carbon dioxide to methane,

$$CO_2(g) + 4H_2(g) \rightarrow CH_4(g) + 2H_2O(g),$$
$$\Delta G^0_{298K} = -27\ \mathrm{kcal\,mol^{-1}},$$

also called the Sabatier reaction [2], is an important catalytic process of fundamental academic interest with potential commercial application [3–5]. Because the interest in the large-scale manufacture of substitute natural gas from the products of coal gasification has greatly diminished in recent decades [6], carbon dioxide methanation has been applied mostly in combination with the methanation of carbon monoxide, such as for the purification of synthesis gas for the production of ammonia. Both carbon dioxide and carbon monoxide are catalyst poisons and must be reduced to <5 ppm before the syngas enters the synthesis section [7]. In addition, the National Aeronautics and Space Administration (NASA) is also interested in applications of the Sabatier reaction for use in future manned space colonization on Mars [4,8]. Bringing Terrene hydrogen to Mars will make it possible to convert the Martian carbon dioxide atmosphere into methane and water for fuel and astronaut life-support systems [8].

Although the CO_2 methanation is thermodynamically favorable ($\Delta G^0_{298K} < 0$), it remains difficult to realize because of the significant kinetic barriers, because this reaction involves an eight-electron reduction. Extensive studies have been carried out on the hydrogenation of carbon dioxide to methane. Various suitable catalytic systems have been tested and studied for this reaction [2–38]. Among group VIII metals, the Ni catalyst has been extensively investigated under widely varying experimental conditions [9–17]. The effect of the support on activity/selectivity and adsorption properties, as well as the kinetic studies focusing on nickel catalysts, have been discussed in detail [15,16,18]. Studies of this reaction on other group VIII metals besides Ni (e.g., supported and unsupported Ru [4,19,21–24], Rh [20,25–30], Pd [31], Pt [19], Ir [19], Os [32], Co [23], and Fe [23,33] catalysts) have been reported.

* Corresponding author.
E-mail address: gary.haller@yale.edu (G.L. Haller).

0021-9517/$ – see front matter
doi:10.1016/j.jcat.2007.03.029

Ruthenium is reportedly the most active catalyst, with the highest selectivity to methane [23,35]; for example, Weatherbee and Bartholomew [23] achieved a CH_4 selectivity of 99.8% with CO_2 conversion of 5.7% at 502 K using Ru/SiO_2 catalyst. Thampi et al. [5] reported nearly 100% selectivity toward CH_4 over Ru/TiO_2 catalyst at low temperature and ambient pressure, along with an enhanced reaction rate, through photoexcitation of the support. However, the photoconversion of CO_2 to methane took a long time, however (∼22 h). Some bimetallic catalyst systems (e.g., $Ni–Mo/Al_2O_3$ [36] and ultrafine Ni(II) ferrite [NF]) [37,38], have been developed, and the interaction between the two metal atoms has been shown to increase catalyst activity and selectivity.

Because the support has a significant influence on the morphology of the active phase, adsorption, and catalytic properties [18], preparation of highly dispersed supported metal catalysts has been the focus of significant research. Solymosi et al. [20] reported a sequence of activity of supported rhodium catalysts of $Rh/TiO_2 > Rh/Al_2O_3 > Rh/SiO_2$. This order of CO_2 methanation activity and selectivity was the same as observed for Ni on the same supports by Vance and Bartholomew [18]. These phenomena can be attributed to the different metal–support electronic interactions, which affects the bonding and the reactivity of the chemisorbed species [20,39].

Previously, we showed that all first-row transition metals can be incorporated into the MCM-41 pore wall while retaining a highly ordered hexagonal structure. With proper pretreatment (reduction), subnanometer-sized metal particles were formed on the pore wall surface of Co-MCM-41 having 100% dispersion and stability under high-temperature reaction in CO [40]. Different pore sizes produced different metal cluster sizes, due to the varying pore radius of curvature of the Co-MCM-41. However, Ni-MCM-41 did not show a measurable radius of curvature effect on the metallic cluster size because of its easier reduction compared with Co-MCM-41. Nevertheless, different reduction temperatures made it possible to control the cluster size and the degree of reduction of Ni [41], which as discusses here, affects the reactivity/selectivity of CO_2 methanation.

In the present work, for the first time C16 Ni-MCM-41 catalysts (with C16 indicating a 16 carbon alkyl template that produces MCM-41 pores of about 2.9 nm diameter) with differing amounts of Ni incorporated during synthesis were applied to CO_2 methanation. The effect of pretreatment conditions was systematically investigated with the aim of devising an effective catalytic system for CO_2 methanation.

2. Experimental

2.1. Materials

The sources of silica were Cab-O-Sil (Cabot) and tetramethylammonium silicate (Aldrich). The nickel source was $Ni(NO_3)_2{\cdot}6H_2O$ (Sigma-Aldrich). Hexadecyl trimethylammonium bromide [$C_{16}H_{33}(CH_3)_3NBr$, Sigma-Aldrich] surfactant was used as a template material. The surfactant solutions were prepared by ion-exchanging the 20 wt% $C_{16}H_{33}(CH_3)_3NBr$ aqueous solution with an equal molar exchange capacity of Amberjet-4400(OH) ion-exchange resin (Sigma) by overnight batch mixing. The antifoaming agent Antifoam A (Sigma), a silane polymer alkyl terminated by methoxy groups. Acetic acid (Fisher Scientific), was used to adjust the pH of the synthesis solution.

2.2. Catalyst

All of the catalysts studied in this work are based on C16 Ni-MCM-41 (16 carbon chain length surfactant; see Ref. [1] for details). The fumed silica Cab-O-Sil (2.5 g) was added into a tetramethylammonium silicate aqueous solution (10.4 g, including 1 g of SiO_2) and stirred vigorously for 30 min. Deionized water (50.7 ml) was added to improve mixing. The nickel aqueous solution [2 wt% $Ni(NO_3)_2{\cdot}6H_2O$] was added and stirred for another 30 min. Two drops of antifoam agent (0.2 wt% of surfactant) were added to this solution, followed by the addition of the surfactant [20 wt% $C_{16}H_{33}(CH_3)_3N{\cdot}OH$] solution (28.7 g). The pH was adjusted to 11.5 by adding acetic acid. The final reactant molar ratios were 0.29 SiO_2 (from $TMA{\cdot}SiO_2$):0.71 SiO_2 (from Cab-O-Sil):0.27 surfactant:0.01 Ni:86 water. After additional mixing for about 120 min, this synthesis solution was poured into a polypropylene bottle and placed in the autoclave at 373 K for 6 days. After cooling to room temperature, the resulting solid was recovered by filtration, washed with deionized water, and dried under ambient conditions. The predried solid was heated at a constant rate from room temperature to 813 K over 20 h under He and held for 1 h under the same condition, followed by calcination at 813 K for 6 h in air to remove the residual surfactant. Because the preparation process can cause some loss of Ni and silica in the byproducts, the final Ni content was determined by ICP analysis at Galbraith Laboratories (Knoxville, TN).

2.3. Catalytic activity test

The catalysts were pretreated in situ in a stream of 15 ml min^{-1} ultrahigh purity H_2 at various conditions before reaction to test the effect of pretreatment at different conditions, i.e., different reduction temperature and reduction time. After reduction, the reduced catalysts were then flushed with ultrahigh purity He for 30 min and cooled to the reaction temperature.

Carbon dioxide methanation was conducted at atmospheric pressure in a fixed-bed down-flow quartz reactor in the temperature range from 373 to 873 K. The thermocouple was directly inserted into the catalyst bed to measure the actual pretreatment and reaction temperature. The reactor was heated in a 127 mm i.d. tube furnace controlled by a PID temperature controller (CN2011J, Omega). All gases were controlled by calibrated mass flow controllers (Brooks).

The H_2 and CO_2 reactants were mixed at H_2:CO_2 ratios ranging from 1 to 4.2, and the gas hourly space velocity (GHSV) was varied from 5760 to 23,000 $l\,kg^{-1}\,h^{-1}$. The feed and products were analyzed by an on-line programmable gas chromatograph (HP 6890) equipped with TCD, Hayesep D column (100/120 mesh, 20 ft), and Hayesep T column (100/120

mesh, 5 ft). The lines from the outlet of the reactor to the GC were heated to 423 K to avoid the condensation of products.

2.4. Characterization

2.4.1. N_2 physical adsorption

Adsorption–desorption isotherms of N_2 at 77 K were measured using a Quanta Chrome Autosorb-1C static volumetric instrument. The pore size and pore size distribution were calculated by the BJH method [42] using the desorption isotherm branch.

2.4.2. CO chemisorption

To investigate the change of metallic particle size of the Ni-MCM-41 catalyst by reduction at different temperature in pure H_2, CO chemisorption was performed in the volumetric static adsorption system (Autosorb-1C, Quanta Chrome), assuming a CO/Ni stoichiometry of 1. A 200-mg 1 wt% Ni-MCM-41 sample was loaded into a quartz flow cell. The reduction was performed at 673, 773, 873, and 973 K for 30 min. After each step, oxygen back-titration at 673 K was carried out to calculate the degree of reduction under the assumption that all metallic Ni was oxidized to NiO.

2.4.3. X-ray diffraction

X-ray diffraction (XRD) measurements were conducted using a Schimadzu X-ray diffractometer (Cu$K\alpha$, $\lambda = 0.154$ nm, 40 kV, 30 mA) to check whether the Ni-MCM-41 samples synthesized in this study have the characteristic hexagonal pore structure, and the same experiment was performed for used catalyst to see whether the structure was maintained after reaction.

2.4.4. X-ray absorption

X-ray absorption data were collected at the Ni K edge (8333 eV) using Si(111) as the monochromator crystal at beam line X23B, National Synchrotron Light Source, Brookhaven National Laboratory. Typically, approximately 100 mg of a given sample was pressed into a self-supporting wafer and placed in a stainless steel cell; incidence and transmission of the X-ray beam were measured by ion chambers filled with pure nitrogen. EXAFS in the transmission mode was recorded from 200 eV below to 900 eV above the Ni K edge. The gas inlet, outlet, and heating and cooling unit allow the in situ treatment of samples and reaction. The local environment of Ni-MCM-41 during CO_2 methanation was monitored in situ by X-ray absorption. The Ni-MCM-41 catalyst (wafer) was first reduced in pure H_2 at 973 K for 30 min, then the reactor was cooled in pure He to room temperature. The reaction was carried out at 473, 573, 673, and 773 K in a reactant flow of H_2:CO_2 (4.0:1) for 30 min. During the reaction period, XANES data were continuously collected from 30 eV below to 50 eV above the Ni K edge, for in situ measurement of the state of the catalyst. EXAFS was measured at room temperature after the sample was cooled from reaction temperatures in He flow.

The spectra thus collected were analyzed using the UWXAFS analysis package [43]. The theoretical EXAFS function for different nickel species (Ni and NiO) generated by the FEFF6 program were used to fit the experimental data to calculate the Ni–Ni and Ni–O first shell coordination numbers [44].

Inductively Coupled Plasma Analysis. The nickel content of each sample was measured by the inductively coupled plasma (ICP) technique at Galbraith Laboratories.

Table 1
Temperature-programmed reaction for CO_2 methanation (catalyst without reduction pretreatment)[a]

Temperature	Conversion (%)		Selectivity (%)		STY of CH_4 ($g\,kg^{-1}\,h^{-1}$)
	H_2	CO_2	CO	CH_4	
373 K	0	0	0	0	0
473 K	0	0	0	0	0
573 K	0.3	0.1	100	0	0
673 K	4.9	8.3	76.6	23.4	30.9
773 K	22.9	35.8	69.0	31.0	187
873 K	34.6	46.5	60.4	39.6	338

[a] Reaction conditions: fresh C16 1 wt% Ni-MCM-41, pretreated with air at 773 K for 1 h, temperature-programmed reaction from 373 to 873 K at H_2:CO_2 = 2.6:1, GHSV of 11,500 $l\,kg^{-1}\,h^{-1}$.

3. Results and discussion

3.1. Preactivation and catalyst state

To investigate the temperature of activation of Ni for CO_2 methanation on Ni-MCM-41, temperature-programmed reaction (TPR) was carried out on 1 wt% Ni-MCM-41 with space velocity of 11,500 $l\,kg^{-1}\,h^{-1}$ and a reactant H_2:CO_2 ratio of 2.6:1 (72% H_2, 28% CO_2) from 373 to 873 K at atmospheric pressure (Table 1). After pretreatment with air at 773 K for 1 h to create the same state with the as-calcined sample and cooling to 373 K under He flow, the feed of H_2 and CO_2 mixture was introduced over Ni-MCM-41 at this temperature without prereduction. Almost no catalytic activity was detected at 373–473 K, and only negligible amounts of products were detected at 573 K. The catalyst began to show significant activity producing CO and CH_4 at 673 K, and the conversion of reactants and selectivity to CH_4 increases further with increasing temperature. A significant fraction of CO was produced, which decreased with increasing temperature. Because the active sites in this reaction are metallic Ni, we can deduce from this result that 673 K is the temperature that Ni-MCM-41 begins to be reduced in the reactant flow and to show catalytic activity, which was further confirmed by our related study by Yang et al. [41] on in situ H_2 reduction of Ni-MCM-41 at different temperatures. In that work, the C16 Ni-MCM-41 samples were reduced under ultra-high purity H_2 for 0.5 h at 673, 773, 873, and 973 K. The Ni–Ni coordination numbers for the samples reduced at different temperatures obtained from analysis of the EXAFS spectra showed that at 673 K, the Ni–Ni coordination number was 2.9, meaning that the Ni in the framework of MCM-41 began to be reduced to Ni atoms associated in a cluster or crystal. At a higher temperature (873 K), the pre-edge peak intensity increased and the Ni–Ni coordination number increased to 5.6, indicating that Ni atoms migrated quickly and formed Ni clusters [41]. The reduction temperature of 673 K was still too low to reduce all of the Ni ions in Ni-MCM-41 (about 9.2% of Ni

reduced as shown in the study of CO chemisorption in Table 2); therefore, the activity increased as the temperature increased, likely due to further reduction of Ni-MCM-41. When the reduction temperature increased to 973 K, the Ni–O coordination number decreased from an initial value of about 4 by about an order of magnitude, showing that a significant amount of Ni in the sample was reduced; this was confirmed by CO chemisorption showing that 72% of Ni was reduced at 973 K (see Table 2). At temperatures above 1073 K, deactivation occurred. This is the temperature at which complete reduction of Ni-MCM-41 is observed by TPR [41], resulting in unconfined rapid migration of Ni out of pores and into large crystals.

The catalytic activity of 1 wt% Ni-MCM-41 catalyst after different reduction pretreatment conditions was studied at 573 K, a H_2:CO_2 ratio of 2.6:1, and GHSVs of 11,500 and 5760 $l\,kg^{-1}\,h^{-1}$, respectively. As shown in Table 3, at low reduction temperatures (673–773 K), with 2–2.5 h of reduction time compared with 0.5 h at high temperature, both the conversions of CO_2 and the selectivities of CH_4 were still very low. When the catalyst was reduced at 973 K for 0.5 h, CH_4 selectivity increased to 85.1% with a space-time yield (STY; defined by the weight of product obtained per unit weight of catalyst and unit time) of 35.6 $g\,kg^{-1}\,h^{-1}$ using 1 wt% Ni-MCM-41 with the GHSV of 5,760 $l\,kg^{-1}\,h^{-1}$. Comparing the selectivities and STYs of CH_4 with Ni-MCM-41 samples reduced at 923 and 973 K for the same reduction time (0.5 h) showed a significant increase in CH_4 selectivity and STY for the sample reduced at 973 K, which was shown to be the best reduction temperature investigated. The analysis of the EXAFS spectra of Ni-MCM-41 samples reduced at different temperature showed that the Ni–Ni coordination number increased systematically with increasing reduction temperature [41]. Low-temperature reduction in hydrogen for 0.5 h gave Ni–Ni coordination numbers of 2.9 for 673 K reduction and 3.5 for 773 K reduction, whereas at 973 K, a significant portion of the Ni was reduced, showing a Ni–Ni coordination number of 7.6. When we consider that these coordination numbers were the volume-averaged values normalized by the total Ni in the sample, containing both reduced and unreduced Ni in MCM-41, and anchoring effects of small metallic clusters discussed elsewhere [40,45], there may not be a substantial difference in the cluster size of Ni between the samples reduced at the lower temperatures until complete reduction resulting in the loss of the anchoring effect and unconfined surface migration. However, without separate normalization of metallic Ni and oxidized Ni, the increased Ni–Ni coordination number would indicate that more Ni ions were reduced, so that more active sites were involved in the reaction. This effect has been studied previously in a related study [46]. Therefore, at 973 K, much of the Ni was reduced, but it remained highly dispersed.

Table 2
CO chemisorption by reducing Ni-MCM-41 at different temperature

Catalysts	Metal surface area[a] ($m^2\,g^{-1}$)	Dispersion[b] (%)	Metal particle size[c] (nm)	Remarks[d]
1 wt% Ni-MCM-41 reduced at 673 K for 0.5 h, CO chemisorption	0.63	100	0.99	9.2% reduced
1 wt% Ni-MCM-41 reduced at 773 K for 0.5 h, CO chemisorption	0.74	69	1.5	18% reduced
1 wt% Ni-MCM-41 reduced at 873 K for 0.5 h, CO chemisorption	2.2	57	1.8	57% reduced
1 wt% Ni-MCM-41 reduced at 973 K for 0.5 h, CO chemisorption	2.9	60	1.7	72% reduced

[a] Metal surface area is in m^2 per gram of catalyst.
[b] Corrected for % reduction by assuming CO/Ni ratio (stoichiometry = 1) of one.
[c] Metal particle shape is assumed to be spherical.
[d] Reduction measured by O_2 back titration at 673 K, assuming $2Ni + O_2 \rightarrow 2NiO$.

The physical stability of Ni-MCM-41 before and after CO_2 methanation was measured by N_2 physisorption and XRD; the results are given in Table 4 and illustrated in Fig. 1. Fig. 1 shows the nitrogen physisorption isotherm of the fresh Ni-MCM-41 catalyst and the catalyst after CO_2 methanation at 573 K and a GHSV of 11,500 $l\,kg^{-1}\,h^{-1}$ for about 7 h. The isotherm of used catalyst retained a steep capillary condensation step of 5710 cc g^{-1} compared with that of the fresh sample of 7330 cc g^{-1}, although the adsorption volume decreased after the reaction due to dehydroxylation. The pore size distribution of both catalysts calculated by the BJH method showed nearly identical narrow, sharp peaks. Apparently, the Ni-MCM-41 catalyst maintained a highly ordered structure.

The BET surface area, the mesopore and total pore volume, and the slope of the capillary condensation of Ni-MCM-41 catalyst decreased after reaction due to the dehydroxylation, as shown in Table 4. However, the pore diameter and the full width at half maximum (FWHM) remained nearly identical for both the used and fresh catalysts. From the XRD patterns illustrated

Table 3
Catalytic activity of 1 wt% Ni-MCM-41 catalyst after different reduction pretreatment[a]

Reduction conditions	GHSV ($l\,kg^{-1}\,h^{-1}$)	Conversion (%)		Selectivity (%)		STY of CH_4 ($g\,kg^{-1}\,h^{-1}$)
		H_2	CO_2	CO	CH_4	
923 K, 0.5 h	11,500	1.1	1.2	44.4	55.6	18.4
973 K, 0.5 h	11,500	2.5	2.1	26.3	73.7	39.5
673 K, 2.0 h	5760	0.5	1.3	68.9	31.1	1.8
773 K, 2.5 h	5760	0.9	1.9	73.6	26.4	2.3
973 K, 0.5 h	5760	6.0	4.7	14.9	85.1	35.6

[a] Reaction conditions: 1 wt% Ni-MCM-41, reduced in pure H_2, reaction temperature 573 K, pressure 1 psi, H_2:CO_2 = 2.6:1.

Table 4
Physical properties of C16 1 wt% Ni-MCM-41 under different conditions

Treatment	BET ($m^2\ g^{-1}$)	Pore diameter (nm)	Mesopore volume ($cc\ g^{-1}$)	Total pore volume ($cc\ g^{-1}$)	Slope of capillary condensation ($cc\ g^{-1}$)	FWHM (nm)
Fresh	1480	2.86	1.29	3.04	7330	0.18
H_2 reduction at 973 K for 0.5 h CO_2 methanation at 573 K for 7 h	1140	2.86	1.01	1.66	5710	0.18

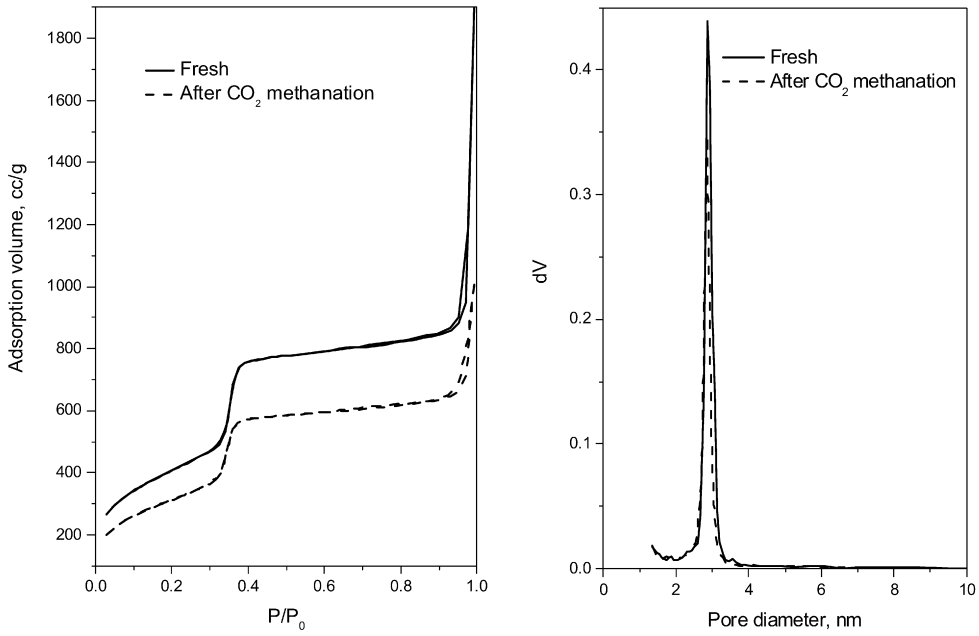

Fig. 1. Nitrogen physisorption adsorption isotherm for C16 1 wt% Ni-MCM-41 catalyst before and after CO_2 methanation.

in Fig. 2, a sharp (100) plane diffraction peak as well as diffraction peaks of higher Miller Index planes (110), (200), and (210) can all be clearly seen for the samples after different pretreatments and CO_2 methanation, demonstrating that the Ni-MCM-41 catalysts synthesized in this study retained a highly ordered hexagonal structure under severe reduction/reaction conditions.

In conclusion, both the nitrogen physisorption and XRD experiments prove that Ni-MCM-41 showed no significant structural change after CO_2 methanation producing substantial amounts of H_2O. This suggests that Ni-MCM-41 synthesized in this study is very stable against hydrothermal degradation.

3.2. *Catalyst state during CO_2 methanation reaction*

To monitor the local environment of Ni in the Ni-MCM-41 catalyst framework, X-ray absorption spectroscopy was carried out in situ under methanation reaction conditions. The C16 1 wt% Ni-MCM-41 catalyst was first reduced from room temperature to 973 K at a rate of 20 K min^{-1} in pure H_2, followed by reduction for 30 min at the same temperature. The in situ XANES were monitored during the process, as shown in Fig. 3. The pre-edge peak intensity and white line intensity are considered the main features for monitoring the reduction of Ni in Ni-MCM-41 [41]. Similar to the H_2 TPR of C12 Ni-MCM-41 [41], the intensity of the white line decreased with an increase in the pre-edge peak intensity during reduction. Note also that the Ni

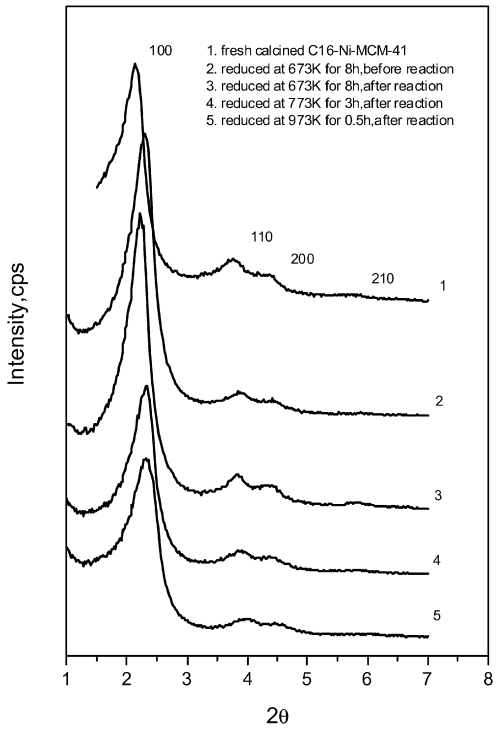

Fig. 2. XRD study of C16 1 wt% Ni-MCM-41 catalyst before and after CO_2 methanation.

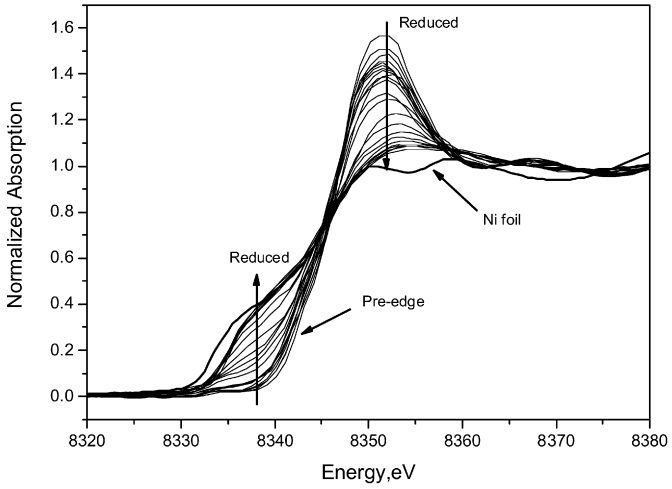

Fig. 3. XANES spectra of in situ H_2 reduction of C16 Ni-MCM-41 at 973 K for 30 min.

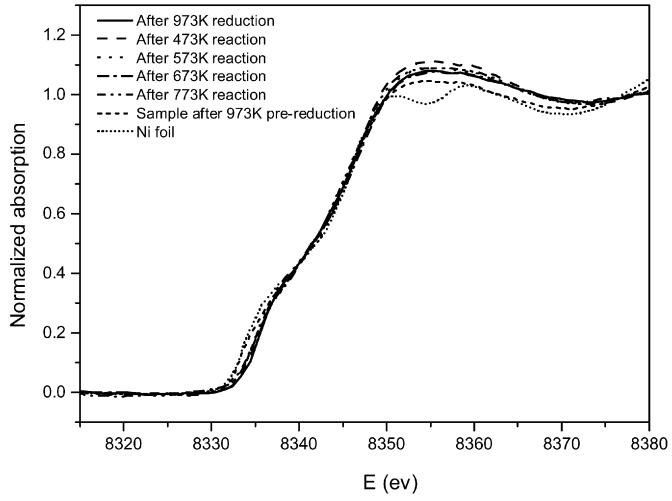

Fig. 4. XANES spectra of C16 1 wt% Ni-MCM-41 sample during in situ CO_2 methanation at different temperature, compared with XANES region of sample after prereduction and Ni foil.

in the framework was not entirely reduced to metal with migration on the surface to form Ni crystallites, showing a difference in the pre-edge peak and white line region compared with that of metal foil.

The prereduced C16 Ni-MCM-41 catalyst was increased to reaction temperatures (i.e., 473, 573, 673, and 773 K) in an atmosphere of H_2:CO_2 = 4.0:1 for 30 min. The pre-edge feature and the white line features of Ni-MCM-41 sample reacted at different temperatures was monitored directly by in situ X-ray absorption, and the spectra were compared with those of prereduced sample and Ni foil, as shown in Fig. 4. A slightly decreased pre-edge peak intensity and a corresponding increase in the white line can be clearly seen for the sample reacting at different reaction temperatures compared with the prereduced sample. At the reaction conditions, a reactant mixture of H_2 and CO_2 (4.0:1) is considered to have relatively low reducing potential compared with that of pure H_2. At this relatively low reducing atmosphere, or on the other hand, in a mild oxidizing

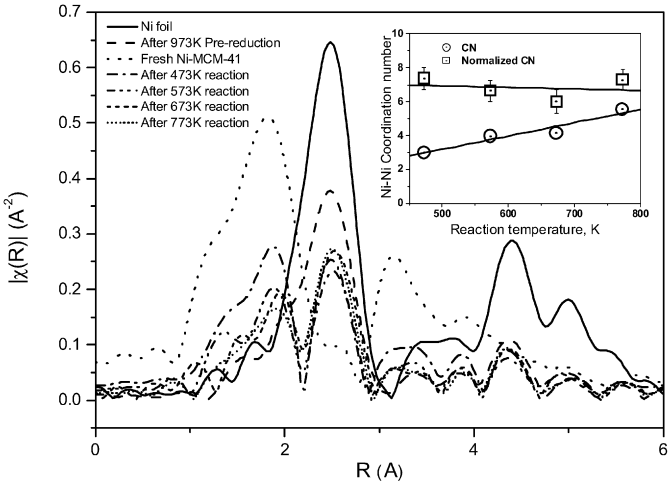

Fig. 5. Fourier transformed k^1-weighted EXAFS of C16 1 wt% Ni-MCM-41 sample after in situ CO_2 methanation at different temperature (inset: normalized Ni–Ni coordination at different temperatures).

atmosphere generated by CO_2, a portion of the Ni metal produced from 973 K H_2 prereduction could be readily oxidized, resulting in a partial oxidation state ($\delta+$) on average.

To investigate the local coordination of Ni-MCM-41 catalyst under reaction conditions, the EXAFS spectra were collected at room temperature after the reactor was purged with pure He. This cooling process inevitably involves partial oxidation of the catalyst at reaction conditions by the He feed (or some potential impurities within the feed) or CO_2 possibly remaining in the reactor chamber, resulting in a partially oxidized pattern, as shown in the spectra in R space (Fig. 5). A Ni–Ni peak at 2–3 Å and a Ni–O peak at 1.5–2 Å can be clearly seem for the samples cooled to room temperature from reaction temperatures. As shown in the inset of Fig. 5, the Ni–Ni coordination number was calculated and normalized by the percentage of oxidation (Ni–O), which was calculated by comparing the Ni–O and Ni–Ni peak intensities of Ni-MCM-41 catalyst during methanation with those of fresh Ni-MCM-41 (assuming 100% Ni–O) and Ni foil (assuming 100% Ni–Ni). There was no significant change in the normalized Ni–Ni coordination number compared with that of 7.6 for the sample after 973 K prereduction [41]. This result indicates that the reduced Ni metal did not seriously migrate on the surface of MCM-41 to form large metal particles or crystallites from 473 to 773 K under reaction conditions.

3.3. Reaction tests at steady states

Because in situ reduction of C16 Ni-MCM-41 with pure H_2 at 973 K for 0.5 h before reaction is the optimum pretreatment condition known to date, all future runs will be based on catalysts pretreated under these conditions. Activity measurements were conducted at 373–873 K, atmospheric pressure, and a GHSV of 5760 to 23,000 $l\,kg^{-1}\,h^{-1}$ using a reaction mixture of H_2 and CO_2 with varying ratios and concentrations. The major products were always methane and carbon monoxide; no C_2 or heavier hydrocarbons were observed in our experiments. Carbon balances were generally >99% of the input carbon. The re-

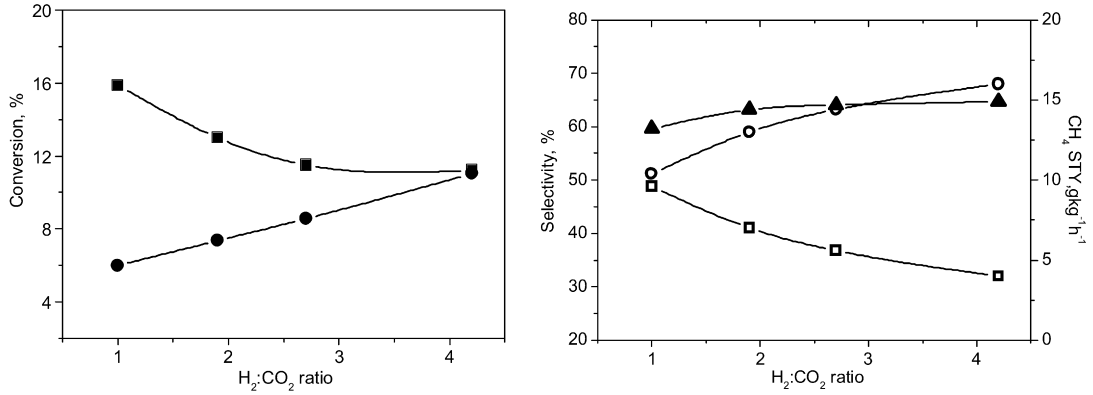

Fig. 6. (a) Dependence of the reactants conversion on their molar ratio. (■) H_2 conversion; (●) CO_2 conversion. (b) Dependence of the products selectivity on the reactants molar ratio. (○) CH_4 selectivity; (□) CO selectivity; (▲) STY of CH_4 (STY = space time yield). 1 wt% Ni-MCM-41, pretreatment with H_2 at 973 K for 0.5 h, reaction temperature 573 K, pressure 1 psi, reactants mole concentration 10%, GHSV 19,200 $l\,kg^{-1}\,h^{-1}$.

Table 5
Catalytic activity and production distribution of Ni-MCM-41 with different space velocity and Ni loading in CO_2 methanation

Sample[a]	Reaction temperature (K)	Conversion (%)		Selectivity (%)		STY of CH_4 ($g\,kg^{-1}\,h^{-1}$)
		H_2	CO_2	CO	CH_4	
1 wt% Ni	573	6.0	4.7	14.9	85.1	35.6
3 wt% Ni	573	11.4	5.6	4.0	96.0	91.4
3 wt% Ni	673	56.0	16.8	3.9	96.1	633

[a] Reduced in pure H_2 at 973 K for 0.5 h, pressure 1 psi, reactant ratio H_2:CO_2 = 2.6:1, GHSV = 5760 $l\,kg^{-1}\,h^{-1}$.

sults reported in this work typically correspond to the catalytic reaction data after the reaction was stabilized for about 2 h.

The H_2:CO_2 catalytic reaction with different ratios was studied at a low reaction temperature (573 K). The reactant ratios were varied by changing the molar fraction of the reactants in the feed at fixed total concentrations of the reactants and a constant space velocity. The conversion of the reactant gases (H_2 and CO_2), the selectivity of the products (CO and CH_4), and the STY of CH_4 at 573 K of 1 wt% C16 Ni-MCM-41 catalysts are shown in Fig. 6. The conversion was defined by molar consumption of the reactant gases, and the selectivity of each product was calculated by the molar ratio of the species of interest to the total amount of carbonaceous product. As shown in Fig. 6, the conversion of CO_2 increased with increasing H_2 partial pressure. The selectivity to CH_4 increased from 51 to 68% with decreasing CO selectivity from 49 to 32% when the H_2:CO_2 ratio was increased from 1 to 4.2. Increasing the H_2:CO_2 ratio produced a positive affect on CH_4 yield, conflicting with the results of Solymosi [35], who found very little influence on the selectivities of Rh catalysts.

The results of CO_2 methanation at low reaction temperature (573 K) using different Ni loadings are given in Table 5. The conversion of the reactants and the selectivity of the methane were increased by keeping the space velocity constant while increasing the Ni loading in Ni-MCM-41. The conversion of the CO_2 and the selectivity of the CH_4 increased by 120% when the Ni loading was increased from 1 to 3 wt%, containing more reduced Ni clusters. The STY of methane produced over 3 wt% Ni-MCM-41 reached 91.4 $g\,kg^{-1}\,h^{-1}$, significantly greater than that on 1 wt% Ni-MCM-41. When the reaction temperature was increased to 673 K, the STY reached 633 $g\,kg^{-1}\,h^{-1}$ (nearly 7 times greater than that of 573 K) with 16.8% CO_2 conversion and a selectivity of 96.1%.

Reactions at different temperatures under steady-state conditions with prereduced C16 Ni-MCM-41 catalysts were also studied. The catalyst was first reduced with pure H_2 at 973 K for 0.5 h, and then activated and stabilized at 573 K for 2 h. The fully activated catalyst was thus ready for use to study the steady-state temperature effect. The selectivity of methane increased with increasing reaction temperature. As shown in Fig. 7, at 573 K the catalyst showed significant methane selectivity (76.7%) and a CO_2 conversion of 3.8% for the reaction at H_2:CO_2 = 2.6:1. Higher catalytic activity was obtained at higher temperatures (673 and 773 K). CO_2 conversion increased with the increased temperature, whereas the selectivity of CH_4 approached its maximum at 673 K. However, for the condition of H_2:CO_2 = 4.0:1, the catalyst already showed a CH_4 selectivity of 56.3% at 473 K, significantly greater than that of catalyst at relatively low reactant ratio. The CH_4 selectivity increased only slightly with the further temperature increase to 773 K. From this observation, it can be deduced that the activation of reaction shifted from high temperature to low temperature due to the increased H_2 concentration, corresponding to a more reducing atmosphere in the reactant feed. The increase of CO_2 conversion with temperature was more pronounced at H_2:CO_2 = 4.0:1, demonstrating improved activity under these conditions. The sustaining of the Ni particle size during CO_2 methanation at different temperatures (inset of Fig. 5) indicates that the increased CH_4 selectivity and CO_2 conversion resulted not from a change in the Ni particle size,

but rather from the effect of temperature, resulting in the different instantaneous selectivity of CH_4 and CO.

The effect of total pressure, an important parameter for the gas-phase reaction, was studied by keeping the reactant ratio and flow rate constant while varying the total pressure of the reaction. As shown in the inset of Fig. 8, CO_2 conversion increased significantly with increasing reaction pressure; for example, an increase from about 3.9 to 7.0% occurred with an increase in pressure from 1 to 25 psi. Meanwhile, the selectivity of CH_4 was observed to increase from 71 to 88%, with a complementary decrease in the selectivity of CO. As a result of the increases in both CO_2 conversion and CH_4 selectivity, the STY of CH_4 increased significantly with increasing pressure.

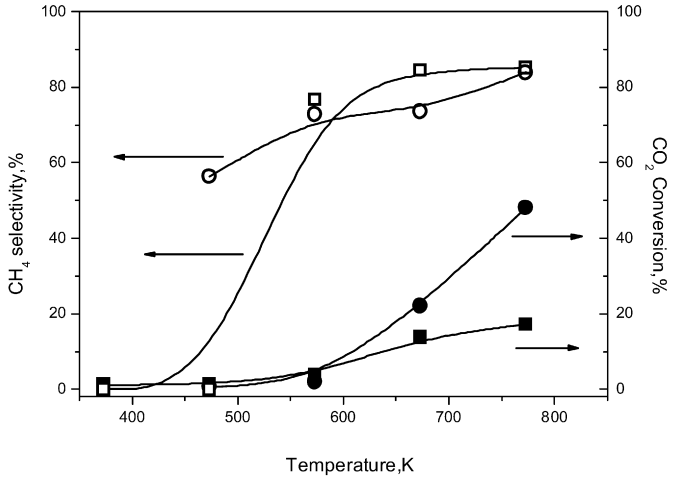

Fig. 7. The selectivity of methane and the conversion of carbon dioxide on the 1 wt% Ni-MCM-41 catalyst at steady state as a function of reaction temperature. (□) CH_4 selectivity, (■) CO_2 conversion at H_2:CO_2 = 2.6:1, GHSV of 11,500 l kg^{-1} h^{-1}, and (○) CH_4 selectivity, (●) CO_2 conversion. H_2:CO_2 = 4.0:1, GHSV of 19,700 l kg^{-1} h^{-1}, for the samples of 1 wt% Ni-MCM-41, prereduced with H_2 at 973 K for 0.5 h.

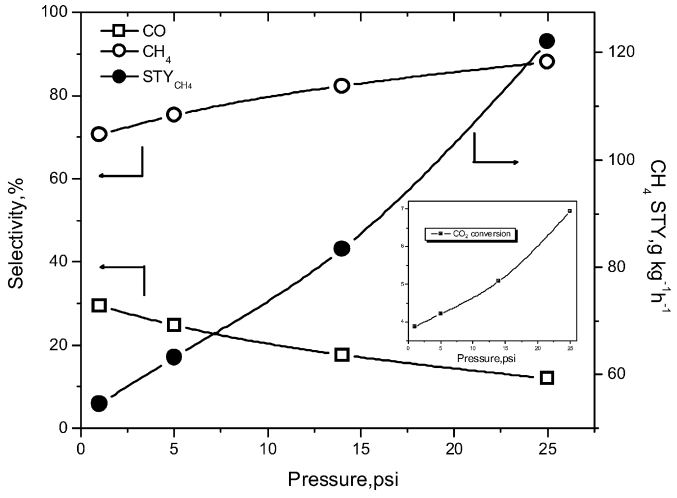

Fig. 8. The reaction pressure effect on carbon dioxide conversion, product selectivities and space time yield of methane over 1 wt% Ni-MCM-41 catalyst reduced with H_2 at 973 K for 0.5 h, at reaction temperature of 573 K, H_2:CO_2 = 4.0:1, and GHSV of 19,700 l kg^{-1} h^{-1}.

3.4. Discussion

For all of the conditions studied, CH_4 selectivities increased with increasing reactant conversion. This suggests that CO_2 methanation on Ni-MCM-41 consists of a sequential reduction and desorbed CO intermediate; this is currently under investigation by kinetic studies.

Increased Ni loading in Ni-MCM-41 catalysts enhanced both the conversion of CO_2 and the selectivity of CH_4. This suggests that at the same pretreatment conditions, more Ni particles were formed in the 3 wt% Ni-MCM-41 than in the 1 wt% Ni-MCM-41, resulting in more active sites for methanation; this was confirmed by Chen's X-ray absorption study on Co loading in Co-MCM-41 catalysts [47]. However, the increases in CO_2 conversion and CH_4 selectivity (120%) were not proportional to the increase in Ni loading (from 1 to 3 wt%).

Because the active sites are the metallic Ni clusters, it is important to reduce the Ni^{2+} to Ni^0 in situ before methanation. By reducing with pure H_2, the Ni^{2+} was reduced to Ni^0, allowing migration from the framework of the MCM-41 to the pore wall surface, as shown in previous results with Co-MCM-41 [48]. In this way, a Ni catalyst with a better dispersion of active sites than the Ni/SiO_2 catalyst likely can be obtained by anchoring Ni to the partially reduced Ni ions on the surface [40,45]. Table 6 compares the activity and selectivity of a typical Ni-MCM-41 catalyst of our work with those of a few silica-supported Ni catalysts studied previously [15,18]. Apparently, the catalyst system in our work exhibits a higher methane selectivity (96%) than the other Ni/SiO_2 catalysts. In addition, due to their high stability, the Ni-incorporated MCM-41 catalysts in our work would be the superior catalyst for the hydrogenation of carbon dioxide to methane. Another summary of the results of methanation of CO_2 on various catalysts can be found elsewhere [17].

Table 6
Comparison of activity and selectivity of carbon dioxide methanation on a variety of catalysts

Catalyst	Temperature (K)	Pressure (kPa)	GHSV (h^{-1})	CO_2 conversion (%)	Selectivity (%)		Reactant feed	Ref.
					CH_4	CO		
3% Ni-MCM-41	573	7	12,700	5.6	96	4	72% H_2, 28% CO_2	[a]
3% Ni/SiO_2	500	140	16,350	3.9	70	9	95% N_2, 4% H_2, 1% CO_2	[15]
3% Ni/SiO_2	525	140	16,350	8.6	77	15	95% N_2, 4% H_2, 1% CO_2	[15]
3% Ni/SiO_2	550	140	32,900	11.2	70	25	95% N_2, 4% H_2, 1% CO_2	[15]
3% Ni/SiO_2, sintered[b]	525	–	3000–70,000	<10	56	44	95% N_2, 4% H_2, 1% CO_2	[18]

[a] This work. For Ni-MCM-41 catalyst, GHSV is 5760 l kg^{-1} h^{-1}; a slightly higher selectivity and 16.8% CO_2 conversion is achieved at 673 K.
[b] Reduced for 16 h in H_2 at 1023 K.

The transient study (TPR) demonstrated that 673 K is the temperature at which Ni-MCM-41 began to be reduced and react in the reactant feed, as demonstrated by CO chemisorption and X-ray absorption for Ni-MCM-41 reduced at different temperatures (see Table 2 and [41]). A prereduced catalyst showed significant activity at 573 K, confirming the importance of prereduction of Ni^{2+} before CO_2 methanation. Reduction at mild temperatures will form small metallic clusters with better dispersion due to less aggregation of Ni clusters. As shown in Table 3, however, reduction at 673 K, even with longer reduction times, was not the optimum catalyst pretreatment. This can be explained by Yang's finding [41] that reduction at temperatures as low as 673 K cannot provide the reduced Ni atoms with sufficient energy to migrate and sinter to form Ni particles, resulting in a small Ni–Ni coordination number of 2.9 with a low degree of reduction. There also may exist a significant occlusion of Ni particles in the silica matrix at low reduction temperature. The reduction temperature for Ni-MCM-41 must be above 873 K to allow formation of Ni clusters with high activity for CO_2 methanation.

Another possible reason for the lower reactivity of catalysts reduced at 873 K compared with those reduced at 973 K may be the partial decoration of the Ni surface by SiO_2 caused by the amorphous structure of the silica forming the framework of MCM-41. Reduction at 973 K for 0.5 h was found to be the best reduction condition for both CO_2 conversion and methane selectivity. At this temperature, most of the Ni was reduced, with a Ni–Ni coordination number of 7.6 [41], however, at higher temperatures (>973 K) corresponding to complete reduction of the Ni resulting in free migration on the surface, catalytic activity was lost. This indicates that the reduction of Ni is initiated at 673 K and produces small Ni clusters that anchor on the unreduced surface Ni ions, limiting migration. At 973 K, most of the Ni will be reduced but will remain anchored to the surface, resulting in the maximum amount of small Ni clusters and highest activity. CO chemisorption showed similar Ni particle sizes with reduction at 773–973 K (Table 2), suggesting that the reduced Ni metal clusters remained anchored on the surface and no serious migration of Ni clusters occurred in this temperature range. At temperatures above 973 K, the anchoring effect will be lost due to the lack of anchoring metal ions in the surface (complete reduction of Ni). The anchoring effect was previously demonstrated for Co-MCM-41 [40,45]. The maintenance of Ni particle size provides another indication of the proposed anchoring effect, which stabilizes the partially reduced Ni during reaction conditions.

4. Conclusion

CO_2 methanation occurred on Ni-MCM-41 at temperatures as low as 573 K, and significant selectivity was demonstrated at this temperature. At high Ni loading (3 wt% Ni), the selectivity reached almost 100%, superior to that of Ni/SiO_2 catalysts and comparable to the best results for Ru/SiO_2 catalysts studied elsewhere. A proper treatment of Ni-MCM-41 provides a method for producing a highly dispersed and thermally stable metallic Ni catalyst. Reduction at 973 K produced the greatest activity and selectivity, and at this temperature, most Ni was reduced to Ni^0, maintaining a high dispersion on the surface without serious aggregation due to the surface anchoring effect. The analysis of EXAFS spectra of Ni-MCM-41 catalyst after reaction demonstrated that Ni particle size did not change significantly under the severe reaction conditions. The catalyst structure did not change much after CO_2 methanation for several hours, producing the high physical stability of this catalytic system.

Acknowledgments

This project was funded by the National Aeronautics and Space Administration (grant NAG 04) and the US Department of Energy, Office of Basic Energy Sciences (grants DE-FG02-01ER15183 and DE-FG02-05ER15732).

References

[1] S. Lim, G.L. Haller, J. Phys. Chem. B 106 (2002) 8437.
[2] P. Sabatier, J.B. Senderens, Acad. Sci. 134 (1902) 689.
[3] A.D. Tomsett, T. Hagiwara, A. Miyamoto, T. Inui, Appl. Catal. 26 (1986) 391.
[4] P.J. Lunde, F.L. Kester, Ind. Eng. Chem. Proc. Des. Dev. 13 (1974) 27.
[5] K.R. Thampi, J. Kiwi, M. Gratzel, Nature 327 (1987) 506.
[6] I. Alstrup, J. Catal. 151 (1) (1995) 216.
[7] B.B. Pearce, M.V. Twigg, C. Woodward, in: M.V. Twigg (Ed.), Catalyst Handbood, second ed., Wolfe Publishing Ltd., London, 1989, pp. 340–383.
[8] D.P. VanderWiel, J.L. Zilka-Marco, Y. Wang, A.Y. Tonkovich, R.S. Wegeng, in: AIChe 2000, Spring National Meeting, Atlanta, GA, 2000.
[9] J.N. Dew, R.R. White, C.M. Sliepcevich, Ind. Eng. Chem. 47 (1955) 140.
[10] L.E. Cratty, W.W. Russell, J. Am. Chem. Soc. 80 (1958) 767.
[11] R. Bardet, M. Perrin, M. Primet, Y. Trambouze, J. Chim. Phys. Phys. Chim. Biol. 75 (1978) 1079.
[12] T. Inui, M. Funabiki, Y. Takegami, React. Kin. Catal. Lett. 12 (1979) 287.
[13] J.A. Dalmon, G.A. Martin, J. Chem. Soc. Faraday Trans. I 75 (1979) 1011.
[14] J.L. Falconer, A.E. Zagli, J. Catal. 62 (1980) 280.
[15] G.D. Weatherbee, C.H. Bartholomew, J. Catal. 68 (1981) 67.
[16] G.D. Weatherbee, C.H. Bartholomew, J. Catal. 77 (1982) 460.
[17] D.E. Peebles, D.W. Goodman, J.M. White, J. Phys. Chem. 87 (1983) 4378.
[18] C.K. Vance, C.H. Bartholomew, Appl. Catal. 7 (1983) 169.
[19] F. Solymosi, A. Erdohelyi, J. Mol. Catal. 8 (1980) 471.
[20] F. Solymosi, A. Erdohelyi, T. Bansagi, J. Catal. 68 (1981) 371.
[21] N.M. Gupta, V.S. Kamble, K.A. Rao, R.M. Iyer, J. Catal. 60 (1979) 57.
[22] E. Zagli, J.L. Falconer, J. Catal. 69 (1981) 1.
[23] G.D. Weatherbee, C.H. Bartholomew, J. Catal. 87 (1984) 352.
[24] S.D. Jackson, R.B. Moyes, P.B. Wells, R. Whyman, J. Chem. Soc. Faraday Trans. I 83 (1987) 905.
[25] B.A. Sexton, G.A. Somorjai, J. Catal. 46 (1977) 167.
[26] T. Iizuka, Y. Tanaka, K. Tanabe, J. Mol. Catal. 17 (1982) 381.
[27] T. Iizuka, Y. Tanaka, K. Tanabe, J. Catal. 76 (1982) 1.
[28] A. Amariglio, M. Lakhdar, H. Amariglio, J. Catal. 81 (1983) 247.
[29] D.W. Goodman, D.E. Peebles, J.M. White, Surf. Sci. 140 (1984) L239.
[30] I.A. Fisher, A.T. Bell, J. Catal. 162 (1996) 54.
[31] A. Erdohelyi, M. Pasztor, F. Solymosi, J. Catal. 98 (1986) 166.
[32] S.D. Jackson, R.B. Moyes, P.B. Wells, R. Whyman, J. Catal. 86 (1984) 342.
[33] D.J. Dwyer, G.A. Somorjai, J. Catal. 52 (1978) 291.
[34] M. Saito, R.B. Anderson, J. Catal. 67 (1981) 296.
[35] F. Solymosi, A. Erdohelyi, M. Kocsis, J. Chem. Soc. Faraday Trans. I 77 (1981) 1003.
[36] A.E. Aksoylu, Z. Misirli, Z.I. Onsan, Appl. Catal. A Gen. 168 (1998) 385.
[37] M. Tsuji, T. Kodama, T. Yoshida, Y. Kitayama, Y. Tamaura, J. Catal. 164 (1996) 315.

[38] T. Kodama, Y. Kitayama, M. Tsuji, Y. Tamaura, Energy 22 (1997) 183.
[39] F. Solymosi, Catal. Rev. 1 (2) (1967) 233.
[40] S. Lim, D. Ciuparu, Y. Chen, Y. Yang, L. Pfefferle, G.L. Haller, J. Phys. Chem. B 109 (2005) 2285.
[41] Y.H. Yang, S. Lim, G.A. Du, Y. Chen, D. Ciuparu, G.L. Haller, J. Phys. Chem. B 109 (27) (2005) 13237.
[42] E.P. Barrett, L.G. Joyner, P.P. Halenda, J. Am. Chem. Soc. 73 (1951) 373.
[43] E.A. Stern, M. Newville, B. Ravel, Y. Yacoby, D. Haskel, Phys. B 209 (1995) 117.
[44] A.L. Ankudinov, B. Ravel, J.J. Rehr, S.D. Conradson, Phys. Rev. B 58 (1998) 7565.
[45] S. Lim, C. Wang, Y. Yang, D. Ciuparu, L. Pfefferle, G.L. Haller, Catal. Today 123 (2007) 122.
[46] Y.H. Yang, S. Lim, G.A. Du, C.A. Wang, D. Ciuparu, Y. Chen, G.L. Haller, J. Phys. Chem. B 110 (2006) 5927.
[47] Y. Chen, D. Ciuparu, S. Lim, G.L. Haller, L.D. Pfefferle, Carbon 44 (2006) 67.
[48] D. Ciuparu, Y. Chen, S. Lim, Y.H. Yang, G.L. Haller, L. Pfefferle, J. Phys. Chem. B 108 (2004) 15565.